Available online at www.sciencedirect.com
ScienceDirect
Trans. Nonferrous Met. Soc. China 25(2015) 1881−1888
Transactions of Nonferrous Metals Society of China
www.tnmsc.cn

Effect of vacuum annealing on microstructure and mechanical properties of TA15 titanium alloy sheets

Hui-jun ZHAO[1], Bao-yu WANG[1], Gang LIU[2], Lei YANG[1], Wen-chao XIAO[1]

1. School of Mechanical Engineering, University of Science and Technology Beijing, Beijing 100083, China;
2. School of Materials Science and Engineering, Harbin Institute of Technology, Harbin 150001, China

Received 9 July 2014; accepted 13 November 2014

Abstract: The mechanical properties, microstructures, and fractographs of TA15 sheets vacuum-annealed under different patterns were investigated. The results indicate that vacuum annealing significantly improves the mechanical properties of the sheets in comparison with those after ambient annealing. With increasing the annealing temperature, the phase boundaries and secondary α-phase increase, whereas the volume fraction of primary α-phase decreases, resulting in increased strength and decreased elongation. A relatively fine secondary α-phase is obtained after double annealing. The desirable mechanical properties (i.e., ultimate tensile strength, yield strength, and elongation are 1070 MPa, 958 MPa, and 15%, respectively) are obtained through double annealing ((950 °C/2 h, AC)+(600 °C/2 h, AC)). The fractographs obtained after tensile tests show that the deepest and largest dimples are formed in the specimen annealed at 850 °C, which indicates that the best plasticity is obtained at this annealing temperature.
Key words: TA15 sheets; vacuum annealing; microstructure; mechanical properties; fractograph

1 Introduction

TA15 (Ti−6Al−2Zr−1Mo−1V) titanium alloy, which possesses high specific strength and good thermal stability, is extensively used to manufacture structural components in the field of aerospace. The alloy is a near-alpha titanium alloy with high aluminum equivalency that exhibits good hot-working plasticity of (α+β) titanium alloys, as well as excellent weldability of α-titanium alloys [1]. A number of researchers have studied the heat treatment and hot deformation behaviors of TA15 alloy [2−10]. ZHU et al [2] investigated the effect of cooling rate on the microstructure evolution during the α/β heat treatment of TA15 titanium alloy. FAN et al [3] determined the influence of heat treatment on the microstructure and damage tolerance property of TA15 alloy. LIU and ZHU [4] studied the effects of triple heat treatment on the stress relaxation resistance of BT20. YANG et al [6] investigated the constitutive behavior and microstructure evolution in hot deformation of TA15 alloy.

However, the reported studies mainly focused on rods and forgings of titanium alloys, whereas studies about titanium alloy plates, especially thin sheets, are rarely reported. LIU et al [11] performed ambient annealing on TA15 sheets at 700−800 °C. They observed that the strength of the sheets decreases, whereas the plasticity of the sheets increases with increasing the annealing temperature. YU et al [12] investigated the hardness of TA15 sheets along three directions after ambient annealing at 740−920 °C. The results showed that the hardness of the sheets annealed at low temperature does not decrease, but the surface of the sheets annealed at high temperature is severely oxidized. The studies about the annealing of TA15 sheets focus on the low temperature range. Oxygen in the dense oxide layer starts to penetrate into the titanium matrix when the heat treatment temperature exceeds 800 °C. The oxide film is broken, and then a gaseous pollution layer forms between the oxide film and the titanium matrix [13]. In general, the gaseous pollution layer exerts adverse impacts on actual mechanical properties of the sheets during ambient annealing. Therefore, titanium alloy sheets often require vacuum annealing.

Compared with ambient annealing, vacuum annealing presents numerous advantages such as anti-oxidation, anti-decarburization, degassing, degreasing, as

Foundation item: Project supported by Beijing Laboratory of Metallic Materials and Processing for Modern Transportation.
Corresponding author: Bao-yu WANG; Tel: +86-10-82375671; E-mail: bywang@ustb.edu.cn
DOI: 10.1016/S1003-6326(15)63795-5

well as relatively fine surface quality and low deformation. Vacuum annealing has been widely applied in titanium alloys as a type of advanced heat treatment technology [14]. Investigating the relationships between the mechanical properties and the microstructural features of titanium alloys after vacuum annealing is necessary.

In this study, several heat treatments were performed to compare vacuum annealing with ambient annealing of TA15 sheets. The mechanical properties and microstructure evolution of sheets that were vacuum annealed under different patterns were studied. The effect of microstructure on the mechanical properties was also analyzed. In addition, the fractographs of tensile specimens after vacuum annealing were investigated.

2 Experimental

The investigated material was a 1.4 mm-thick cold-rolled TA15 sheet. The chemical compositions of the alloy are (mass fraction): 6.67% Al, 1.18% Mo, 1.41% V, 1.97% Zr, 0.075% O, 0.0087% N, 0.0052% H, Ti balance. The β transus temperature is approximately 990 °C.

The recrystallization temperature of TA15 is 800−950 °C. For titanium alloys, in general, the normal annealing temperature is equal to or slightly below the recrystallization temperature. The recrystallization annealing temperature ranges between the recrystallization temperature and the β transus temperature. For double annealing, the first annealing temperature is not below the recrystallization temperature, whereas the second annealing temperature is below the recrystallization temperature [15]. The processes involved in vacuum annealing are shown in Table 1. For comparison, the processes of ambient annealing are also shown in Table 1.

Table 1 Annealing process performed on TA15 sheets

Vacuum annealing No.	Ambient annealing No.	Annealing pattern	Annealing processes
A1	a	Normal annealing	750 °C/2 h, AC
A2	–		800 °C/2 h, AC
B1	b1	Recrystallization annealing	850 °C/2 h, AC
B2	–		900 °C/2 h, AC
B3	–		930 °C/2 h, AC
B4	b2		950 °C/2 h, AC
C1	–	Double annealing	(930 °C/2 h, AC) + (600°C/2 h, AC)
C2	c		(950 °C/2 h, AC) + (600 °C/2 h, AC)

The heat treatments were performed in a chamber electric furnace. The specimens used for vacuum annealing were sealed in quartz glass tubes under a vacuum degree of 10^{-5} MPa, whereas the specimens used for ambient annealing were coated with a high temperature antioxidant, Ti2, as shown in Fig. 1.

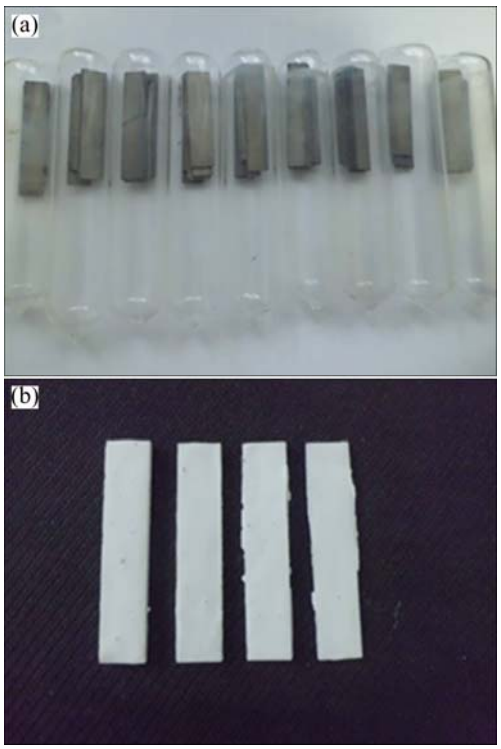

Fig. 1 Specimens of TA15 before vacuum annealing (a) and ambient annealing (b)

After annealing, all of the specimens were machined by wire-electrode cutting for the tensile tests and simultaneously cut perpendicular to the rolling direction for the metallographic examination. Figure 2 shows the dimensions of the specimens used for the tensile tests. The tensile tests were performed (for three times) on a CMT4105 microcomputer electronic universal testing machine at room temperature. The microstructures of the specimens were observed using a JSM−6510A scanning electron microscope (SEM) and a TECNAI G2 transmission electron microscope (TEM). Meanwhile, the elemental compositions of each phase were detected using a JSM−6510A energy-dispersive

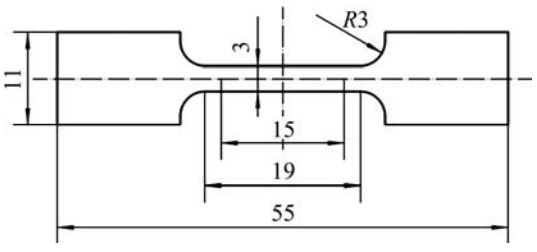

Fig. 2 Dimensions of specimens used in tensile test (Unit: mm)

spectrometer (EDS). The quantitative metallographic analysis was performed by Image-Pro Plus. The fractographs of the tensile specimens were observed by SEM.

3 Results and discussion

3.1 Mechanical properties

The ultimate tensile strength and elongation of the TA15 sheets after vacuum annealing and ambient annealing are shown in Fig. 3. Compared with ambient annealing, the ultimate tensile strength and elongation of the alloy are significantly increased by vacuum annealing. For example, the ultimate tensile strength increases by 1.8%−14.5%, and the elongation increases by 26.3%−642.3%. Meanwhile, with increasing the annealing temperature or multiple annealing, more considerable differences in mechanical properties are observed between the samples under vacuum annealing and ambient annealing. This finding indicates that the anti-oxidation of vacuum annealing at elevated temperature is highly significant. Hence, investigating the effect of vacuum annealing on the mechanical properties of TA15 alloy sheets is necessary.

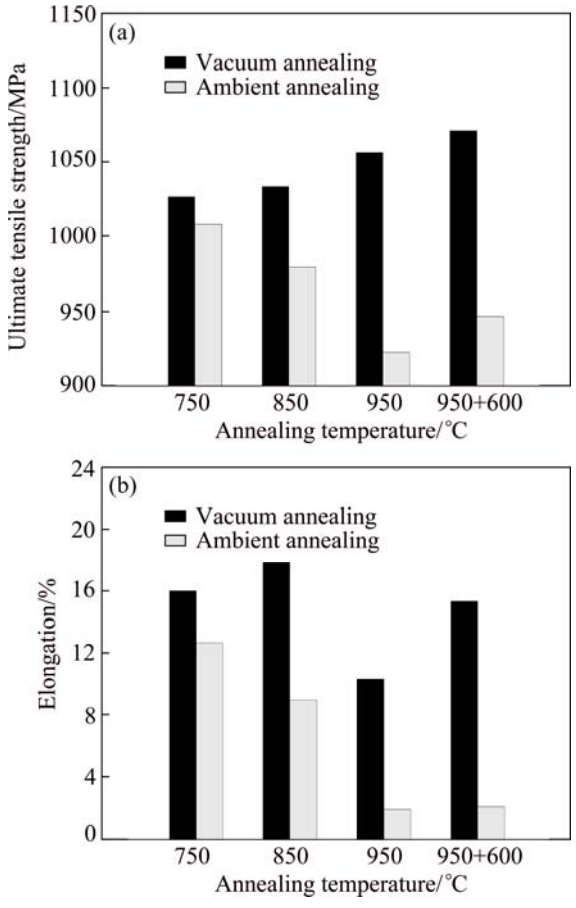

Fig. 3 Mechanical properties of TA15 sheets after vacuum annealing and ambient annealing: (a) Ultimate tensile strength; (b) Elongation

Figure 4 shows the tensile properties of TA15 sheets that were vacuum-annealed in different processes. The alloy presents good mechanical properties after vacuum annealing. Besides the 10.3% elongation of the sheets vacuum-annealed at 950 °C, the ultimate tensile strength, yield strength, and elongation of all other vacuum-annealed sheets reach 1025 MPa, 885 MPa, and 13%, respectively. In general, the comprehensive mechanical properties of vacuum-annealed sheets are better than those of as-received sheets.

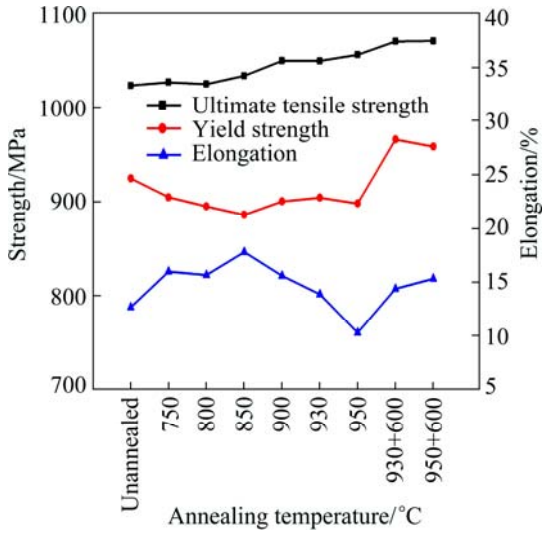

Fig. 4 Mechanical properties of vacuum-annealed TA15 sheets in different processes

As shown in Fig. 4, the vacuum-annealed sheets possess higher ultimate tensile strength than the as-received sheets. The ultimate tensile strength increases with increasing the annealing temperature, but compared with the as-received sheets, its growth is below 5%.

With increasing the annealing temperature, the elongation of the sheets increases, whereas the yield strength of the sheets decreases after normal annealing (750 °C and 800 °C). Compared with normal annealing, the higher elongation of 17.8% and lower yield strength of 886 MPa are obtained through annealing at 850 °C. However, with increasing the annealing temperature, the elongation of the sheets decreases, whereas the yield strength of the sheets increases after recrystallization annealing (850−950 °C).

The strength and plasticity of the sheets after double annealing are higher than those after single annealing. For example, compared with single annealing (950 °C/2 h, AC), after double annealing ((950 °C/2 h, AC) + (600 °C/2 h, AC)), the ultimate tensile strength, yield strength, and elongation of the sheets increase by 1.4%, 6.7%, and 48.7%, respectively. It is found that good comprehensive mechanical properties are obtained through double annealing ((950 °C/2 h, AC) + (600 °C/

2 h, AC)), the ultimate tensile strength, yield strength, and elongation of the TAl5 sheets are 1070 MPa, 958 MPa, and 15%, respectively.

3.2 Microstructural analysis

The microstructures of TA15 sheets vacuum-annealed via different processes are shown in Fig. 5. The volume fractions of primary α-phase (α_p) were quantitatively determined by Image-Pro Plus, as shown in Fig. 6.

As shown in Fig. 5(a), the original microstructure consists of an α-matrix and a grain boundary β-phase. The grains are broken, and parts of these grains are elongated into strips. The microstructure does not change significantly, but the volume fraction of elongated grains reduces after annealing at 750 °C (Fig. 5(b)) and 800 °C (Fig. 5(c)). The recovery decreases the vacancy concentration, and several polygonal microstructures appear, and then the substructure is formed [16]. The internal stress generated in the rolling process can be partially eliminated. This effect increases the elongation and decreases the yield strength of the sheets after normal annealing, compared with those of the as-received sheets.

Figures 5(d)−(g) show the microstructural changes and the contents of α- and β-phases after recrystallization annealing, during which recrystallization and phase transition occur simultaneously.

Recrystallization evidently occurs at 850 °C (Fig. 5(d)). The process can eliminate defects, such as pile-up dislocation, and completely eliminate the internal stress of the sheets. Compared with normal annealing, higher elongation and lower yield strength are obtained through annealing at 850 °C.

At annealing temperature higher than 900 °C, the microstructures start to become bimodal (Figs. 5(e)−(g)). With increasing the annealing temperature, the volume fraction of β-phase increases. Thus, the α/β boundaries increase, and the strength of boundaries is improved. In addition, the secondary α-phase (α_s) precipitates from β-phase. The fine α_s produces a dispersion strengthening effect [17]. However, the grains grow with increasing the annealing temperature, which reduces the phase boundary area and diminishes the strengthening because of phase transformation. This finding also explains why the ultimate tensile strength of the sheets moderately increases with increasing the annealing temperature.

In addition, the plasticity of the sheets decreases with increasing the annealing temperature after recrystallization annealing. The elongation decreases from 17.8% (at 850 °C) to 10.3% (at 950 °C) (Fig. 4). Two reasons explain this result. First, the effect of α_p, by

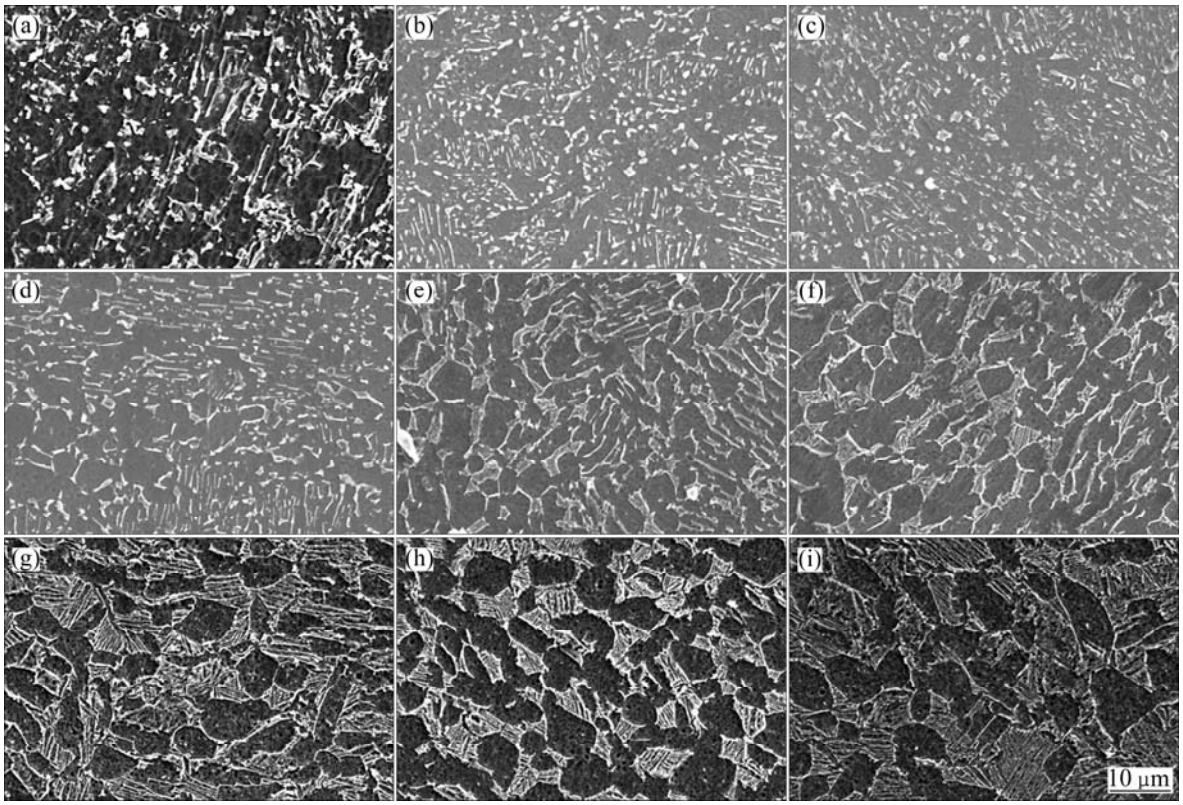

Fig. 5 SEM images of TA15 alloy after vacuum annealing under different conditions: (a) Original microstructure; (b) 750 °C/2 h, AC; (c) 800 °C/2 h, AC; (d) 850 °C/2 h, AC; (e) 900 °C/2 h, AC; (f) 930 °C/2 h, AC; (g) 950 °C/2 h, AC; (h) (930 °C/2 h, AC)+(600 °C/2 h, AC); (i) (950 °C/2 h, AC)+(600 °C/2 h, AC)

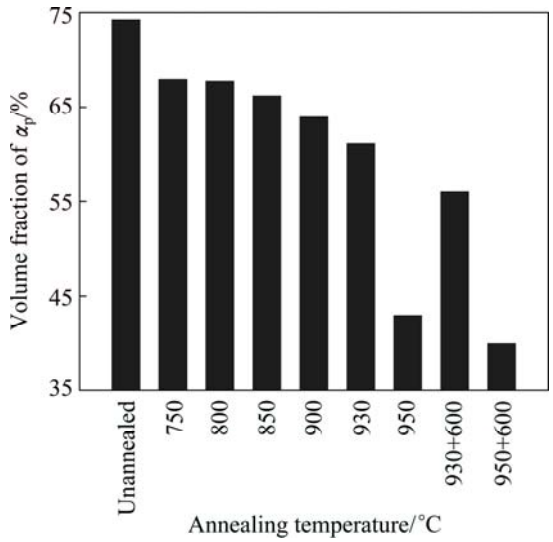

Fig. 6 Volume fractions of α_p in TA15 sheets vacuum-annealed under different processes

which the volume fraction of α_p gradually decreases with increasing the annealing temperature. Figure 6 shows that the volume fraction of α_p reduces from 74% (unannealed) to 60%−70% (annealed at 750–930 °C). The change is not significant. However, the volume fraction of α_p significantly reduces from 61% (at 930 °C) to 43% (at 950 °C), indicating that the volume fraction of α_p is highly sensitive to the annealing temperature, which is near the β transus temperature. The tensile deformation of the bimodal microstructure starts from the slip of several α_p grains. An increasing number of α_p grains begin to slip and expand to the transformed β microstructure (β_t) during deformation. More α_p grains are retained at low annealing temperature, thereby reducing the mean free path of α_p and the spacing of slip band, resulting in evenly distributed dislocation and reduced stress concentration [18]. Therefore, higher elongation is obtained.

Second, such trend is affected by α_s. The deformation of β_t first occurs in β-phase and gradually spreads to α_s. Meanwhile, the α/β boundaries present a near-Burgers orientation relationship ($(0001)_\alpha // (101)_\beta$ and $[2\bar{1}\bar{1}0]_\alpha // [\bar{1}\bar{1}\bar{1}]_\beta$), and thus, only dislocations that slip along the $(101)_\beta[\bar{1}\bar{1}\bar{1}]_\beta$ slip system in the β-phase can easily cross the α/β boundaries [17]. Plastic deformation is more difficult in a lamellar structure than in a primary α-phase. The volume fraction of β_t increases with increasing the annealing temperature, and thus the elongation of the sheets decreases. Furthermore, LÜTJERING [19] considered that the size diminution of the lamella α-phase is conducive to improving the elongation of the material. The α_s is nearly not observed in the microstructures of sheets after annealing at 750−850 °C (Figs. 5(b)−(d)). At annealing temperature exceeding 900 °C, α_s is observed and its thickness increases with increasing the annealing temperature (Figs. 5(e)−(g)). The thickness of α_s is approximately 0.19 μm after annealing at 900 °C, whereas the thickness reaches approximately 0.34 μm at 930 °C and 0.52 μm at 950 °C. Therefore, the volume fraction and thickness of α_s increase with increasing the annealing temperature, resulting in the decreased elongation of the sheets.

The chemical compositions of each phase of the alloy that was vacuum-annealed via different processes were detected by EDS (Table 2). For each specimen, the Al content in α_p is higher than that in β_t, while the V and Mo contents are significantly lower. With increasing the annealing temperature, the Al content increases in β_t, whereas the V and Mo contents decrease in β_t. These findings indicate that the solubilized Al element in the α-phase has diffused into the β-phase. With increasing the temperature, the diffusion coefficient of Al element increases, resulting in increased transformation rate of α_p into β. Meanwhile, the stability of β-phase decreases as the β-stable elements (V and Mo) in β-phase are diminished. This effect is conducive to the transformation from β to α_s in the process of air cooling (AC), thus, the volume fraction of α_s increases [20, 21]. This result is consistent with the results shown in Figs. 5 and 6.

Table 2 Mass fraction of elements in each phase after vacuum annealing

Annealing processes	Phase	Mass fraction/%				
		Ti	Al	V	Zr	Mo
Unannealed	α_p	79.75	6.93	1.90	1.71	0.37
	β_t	54.17	2.08	6.14	1.12	12.78
750 °C/2 h, AC	α_p	76.29	6.18	1.79	1.67	0.28
	β_t	61.56	3.32	3.92	1.40	7.31
800 °C/2 h, AC	α_p	77.46	6.09	2.23	1.82	0.40
	β_t	65.91	3.88	3.71	1.67	5.43
850 °C/2 h, AC	α_p	77.28	6.17	1.80	1.69	0.30
	β_t	67.43	3.98	3.67	1.77	4.20
900 °C/2 h, AC	α_p	74.26	6.11	1.50	1.61	0.29
	β_t	67.26	4.10	3.36	2.06	2.93
930 °C/2 h, AC	α_p	74.94	6.12	1.76	1.54	0.18
	β_t	65.47	4.18	3.09	1.68	2.81
950 °C/2 h, AC	α_p	68.34	6.15	1.29	1.31	0.24
	β_t	59.58	4.51	2.87	1.79	2.46
(930 °C/2 h, AC)+ (600 °C/2 h, AC)	α_p	67.16	6.61	1.15	1.46	0.27
	β_t	60.29	4.41	2.21	1.59	1.84
(950 °C/2 h, AC)+ (600 °C/2 h, AC)	α_p	68.14	6.35	1.41	1.34	0.25
	β_t	62.90	4.34	2.09	1.66	1.36

The TEM images of the samples after single annealing (950 °C/2 h, AC) and double annealing ((950 °C/2 h, AC)+(600 °C/2 h, AC)) are shown in Fig. 7.

The thickness of α_s is approximately 0.52 μm after single annealing, whereas after double annealing that is 0.43 μm. Thus, the secondary α-phase in β_t is finer after double annealing. As shown in Table 2, the V and Mo contents in β_t after double annealing are lower than those after single annealing, thus, more α_s is precipitated. This result can be attributed to the retention of metastable β-phase after first annealing, which can be fully decomposed after second annealing [13]. The finer and more dispersive α_s results in a more evident and frequent change of propagation direction of cracks after the onset of cracking. Hence, the propagation of cracks needs to overcome a greater resistance [22]. In addition, it can be seen by comparing Figs. 7(a) and (b) that the finer α_s reduces the spacing of slip band and pile-up dislocation in the α/β boundaries, thus, the stress concentration is reduced and the deformation becomes more uniform [23]. As a result, the strength and plasticity of the alloy are improved after double annealing.

3.3 Fractograph characteristics

The fractographs of the vacuum-annealed samples after tensile tests are shown in Fig. 8. Figure 8 exhibits evident ductile fracture with numerous dimples. Given the better coordination capability of deformation of α_p than that of β_t, the slip of dislocation occurs from α_p to β_t. In addition, given that the volume fraction of α_p is relatively high after annealing at 750−850 °C, the deformation can quickly spread to more α_p grains, thus reducing the stress concentration [15]. Moreover, with increasing the annealing temperature, the dimples become deeper and larger (Figs. 8(a)−(c)). This is because of recovery even recrystallization, which generates more slip systems. Therefore, the plasticity of the alloy is improved. The largest and deepest dimples are found in the samples annealed at 850 °C, and such dimples indicate that the plasticity of the sheets is the best under this condition.

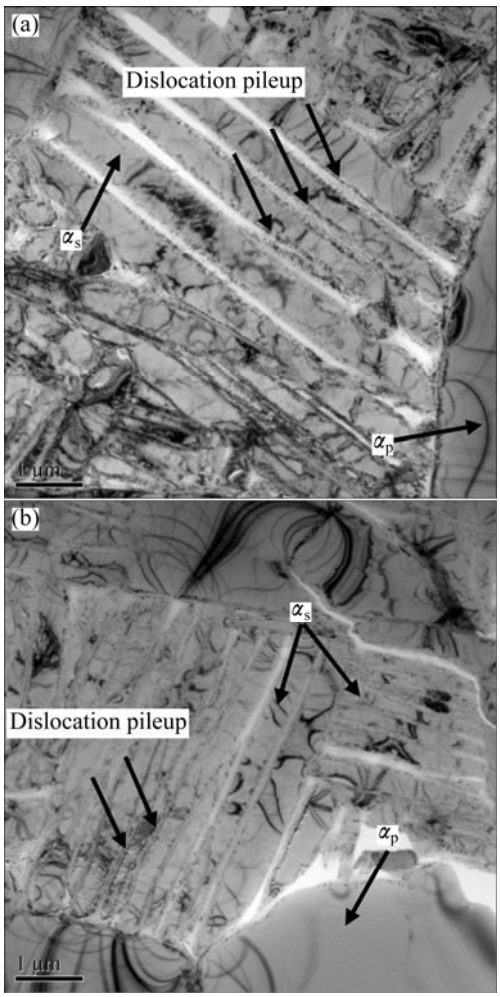

Fig. 7 TEM images of TA15 alloy after single annealing and double annealing: (a) 950 °C/2 h, AC; (b) (950 °C/2 h, AC) + (600 °C/2 h, AC)

When the annealing temperature exceeds 850 °C, the quantity and depth of dimples decrease (Figs. 8(d) and (e)) because the volume fraction of α_p decreases and α_s starts to precipitate from the β-phase. The increased phase boundaries impede the slip, resulting in more difficult deformation of the alloy. Figure 8(e) shows decreased dimples and evident river-like tearing ridges, and the fractograph resembles a quasi-cleavage fracture. This result indicates that the plasticity of the alloy is the lowest after annealing at 950 °C, because thick colonies of α_s strongly impede the slip and the dislocations hardly cross the α/β boundaries, as shown in Fig. 7(a). The stress concentration occurs in the phase boundaries, inducing specimens to enter the yield stage earlier [15].

However, as shown in Fig. 8(f), the dimples are more numerous and deeper after double annealing ((950 °C/2 h, AC) + (600 °C/2 h, AC)). With more abundant and finer secondary α-phase, the pile-up dislocation in the α/β boundary is reduced (Fig. 7(b)). The deformation disperses to more grains and becomes uniform, thereby increasing the plastic deformation before fracture. In general, the fractographs are consistent with the plasticity trend of the sheets observed in Fig. 4.

4 Conclusions

1) Vacuum annealing significantly improves the mechanical properties of the sheets in comparison with those after ambient annealing. The ultimate tensile strength increases by 14.5%, and the elongation increases by 642.3% after double annealing ((950 °C/2 h, AC) + (600 °C/2 h, AC)).

2) The microstructures and mechanical properties of TA15 sheets that were vacuum-annealed under different patterns are affected by recovery, recrystallization, and phase transition. With increasing the annealing temperature, the phase boundaries and secondary

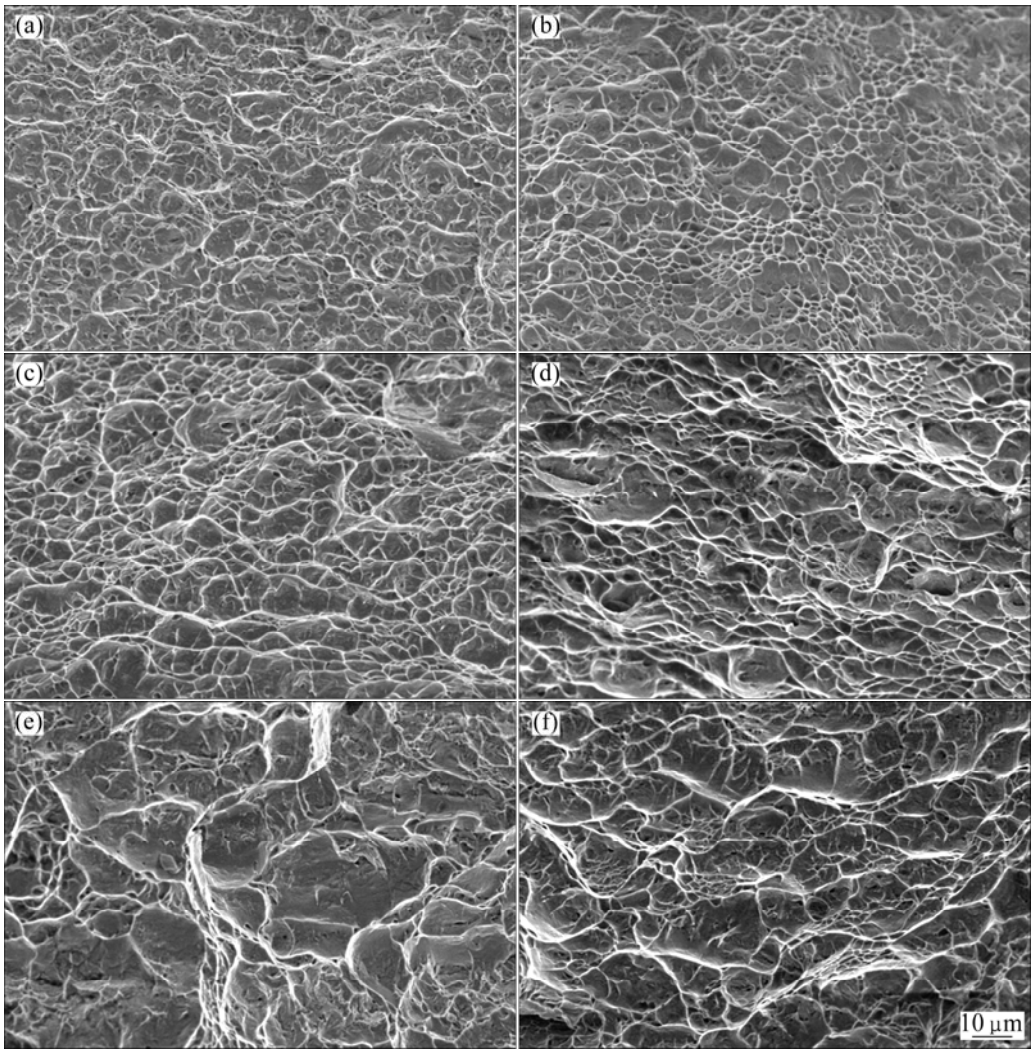

Fig. 8 SEM images of fractures after vacuum annealing: (a) 750 °C/2 h, AC; (b) 800 °C/2 h, AC; (c) 850 °C/2 h, AC; (d) 900 °C/2 h, AC; (e) 950 °C/2 h, AC; (f) ((950 °C/2 h, AC)) + ((600 °C/2 h, AC))

α-phase increase, whereas the volume fraction of primary α-phase decreases. Thus, the strength of the sheets increases, and the elongation of the sheets decreases.

3) The mechanical properties of the sheets after double annealing are improved in comparison with those after single annealing, because a finer and more dispersive secondary α-phase are obtained after double annealing, thereby reducing the spacing of slip band and pile-up dislocation in the α/β boundaries. Good comprehensive mechanical properties are obtained through double annealing ((950 °C/2 h, AC)+(600 °C/2 h, AC)), in which the ultimate tensile strength, yield strength, and elongation are 1070 MPa, 958 MPa, and 15%, respectively.

4) The fractographs of TA15 after vacuum annealing predominantly show ductile fracture, and that of the specimen vacuum-annealed at 950 °C resembles a quasi-cleavage fracture. The sheets that were vacuum-annealed at 850 °C have the best plasticity, exhibiting the deepest and largest dimples.

References

[1] LI Fu-guo, YU Xiao-lu, JIAO Lei-kui, WANG Qiong. Research on low cycle fatigue properties of TA15 titanium alloy based on reliability theory [J]. Material Science and Engineering A, 2006, 430: 216−220.

[2] ZHU Shuai, YANG He, GUO Liang-gang, FAN Xiao-guang. Effect of cooling rate on microstructure evolution during α/β heat treatment of TA15 titanium alloy [J]. Materials Characterization, 2012, 70: 101−110.

[3] FAN Rong-hui, ZHU Ming, HUI Song-xiao, LI De-fu, SHEN Jian. Influence of heat treatment on microstructure and damage tolerance property in Ti−6Al−2Zr−1Mo−1V [J]. Transactions of Nonferrous Metals Society of China, 2007, 17: 482−485.

[4] LIU Yong, ZHU Jing-chuan. Effects of triple heat treatments on stress relaxation resistance of BT20 alloy [J]. Mechanics of Materials, 2008, 40(10): 792−795.

[5] HUANG De-ming, WANG Huai-liu, CHEN Xin, CHEN Yong, GUO Hua. Influence of forging process on microstructure and mechanical properties of large section Ti−6.5Al−1Mo−1V−2Zr alloy bars [J].

Transactions of Nonferrous Metals Society of China, 2013, 23: 2276−2282.
[6] FAN Xiao-guang, YANG He, GAO Peng-fei. Prediction of constitutive behavior and microstructure evolution in hot deformation of TA15 titanium alloy [J]. Materials and Design, 2013, 51: 34-42.
[7] FILIP R, KUBIAK K, ZIAJIA W. The effect of microstructure on the mechanical properties of two-phase titanium alloys [J]. Journal of Materials Processing Technology, 2003, 133: 84−89.
[8] OUYANG De-lai, WANG Ke-lu, CUI Xia. Dynamic recrystallization of Ti−6Al−2Zr−1Mo−1V in β forging process [J]. Transactions of Nonferrous Metals Society of China, 2012, 22: 761−767.
[9] CHEN Yong, XU Wen-chen, SHAN De-bin, GUO Bin. Microstructure evolution of TA15 titanium alloy during hot power spinning [J]. Transactions of Nonferrous Metals Society of China, 2011, 21: 323−327.
[10] XU Wen-chen, SHAN De-bin, LU Yan, LI Chun-feng. Research on the characteristics of hot deformation in BT20 titanium alloy and its optimum spinning temperature range [J]. Journal of Materials Science and Technology, 2005, 21(6): 807−812.
[11] LIU Rui-min, LI Xing-wu, SHA Ai-xue. The study of the microstructure and properties of TA15 titanium ally plate [J]. Development and Application of Materials, 2005, 20(4): 23−25. (in Chinese)
[12] YU Zhong-liang, DONG Jian, XIE Li, WANG De-qin. Effect of annealing process on three directions hardness and microstructure of TA15 titanium alloy sheet [J]. Heat Treatment of Metals, 2011, 36(11): 73−75. (in Chinese)
[13] ZHANG Zhu, WANG Qun-jiao, MO Wei. Titanium metallography and heat treatment [M]. Beijing: Metallurgical Industry Press, 2009: 211−212. (in Chinese)
[14] YAN Cheng-pei. Vacuum and controlled atmosphere heat treatment [M]. Beijing: Chemical Industry Press, 2006. (in Chinese)
[15] ZHAO Yong-qing, CHEN Yong-nan, ZHANG Xue-min, ZENG Wei-dong, WANG Lei. Phase transformation and heat treatment of titanium alloys [M]. Changsha: Central South University Press, 2012: 126−140. (in Chinese)
[16] ZHANG Xi-yan, ZHAO Yong-qing, BAI Chen-guang. Titanium alloys and their applications [M]. Beijing: Chemical Industry Press, 2005: 102−104. (in Chinese)
[17] WANG Tao, GUO Hong-zhen, WANG Yan-wei, PENG Xiao-na, ZHAO Yan, YAO Ze-kun. The effect of microstructure on tensile properties, deformation mechanisms and fracture models of TG6 high temperature titanium alloy [J]. Material Science and Engineering A, 2011, 528: 2370−2379.
[18] DUAN Rui, CAI Jian-ming, LI Zhen-xi. Effect of primary α phase volume fraction on tensile property and thermal stability of near-alpha TG6 titanium alloy [J]. Journal of Aeronautical Material, 2007, 27(3): 17−21. (in Chinese)
[19] LÜTJERING G. Influence of processing on microstructure and mechanical properties of (α+β) titanium alloys [J]. Materials Science and Engineering A, 1998, 243: 32−45.
[20] LEYENS C, PETERS M. Titanium and titanium alloys [M]. Weinheim: Wiley, 2006.
[21] WANG Yong-ling, SONG Xiao-yun, MA Wen, ZHANG Wen-jing, YE Wen-jun, HUI Song-xiao. Microstructure and tensile properties of Ti-62421S alloy plate with different annealing treatments [J]. Rare Metals, 2014, doi: http://dx.doi.org/10.1007/s12598-014−0349-5.
[22] GUO Zhi-jun, WANG Jian, REN Lian-bao, WANG Hong-wu, GUO Hong-bo, WEI Shou–yong. Microstructure and properties of Ti−6Al−2Zr−1Mo−1V alloy plate [J]. Acta Metallurgica Sinica, 2002, 38(s1): 186−187. (in Chinese)
[23] ZHU Zhi-shou. Research and development of new-brand titanium alloys of high performance for aeronautical applications [M]. Beijing: Aviation Industry Press, 2013: 51−59. (in Chinese)

真空退火对 TA15 合金板材组织和力学性能的影响

赵慧俊[1]，王宝雨[1]，刘 钢[2]，杨 雷[1]，校文超[1]

1. 北京科技大学 机械工程学院，北京 100083；
2. 哈尔滨工业大学 材料科学与工程学院，哈尔滨 150001

摘 要：研究 TA15 板材在不同条件下真空退火后的力学性能、显微组织和断口形貌。结果表明：相比非真空退火，真空退火显著提高板材的力学性能。随着退火温度的升高，相界面和次生 α 相增多，但初生 α 相体积分数减少，从而导致板材的强度提高，伸长率降低。双重退火后获得的次生 α 相更加细小。在(950 °C/2 h, AC)+(600 °C/2 h, AC)下双重退火获得了良好的力学性能，其抗拉强度、屈服强度和延伸率分别为 1070 MPa, 958 MPa 和 15%。从拉伸断口形貌可以看到，最深最大的韧窝出现在 850 °C 退火试样上，说明在该温度下退火板材塑性最好。

关键词：TA15 板材；真空退火；显微组织；力学性能；断口形貌

(Edited by Mu-lan QIN)